


# Image Cover Sheet

<b>CLASSIFICATION</b>  UNCLASSIFIED	<b>SYSTEM NUMBER</b> 516676 
---	--

**TITLE**  
Investigation of crack turning in fracture in ship structures

**System Number:**  
**Patron Number:**  
**Requester:**

**Notes:**

<b>DSIS Use only:</b>  <b>Deliver to:</b> CL
--

This page is left blank

This page is left blank



## **Investigation of Crack Turning in Fracture in Ship Structures**

*D.R. Smith  
Suite 707  
5959 Spring Garden Road  
Halifax, Nova Scotia*

*Contract No W7707-0-8234/001/HAL*

**Defence Research Establishment Atlantic**

**Defence R&D Canada**

Contractor Report

DREA CR 2001-067

July 2001

## **REPRODUCTION QUALITY NOTICE**

**This document is the best quality available. The copy furnished to DRDCIM contained pages that may have the following quality problems:**

**: Pages smaller or Larger than normal**

**: Pages with background colour or light coloured printing**

**: Pages with small type or poor printing; and or**

**Pages with continuous tone material or colour photographs**

**Due to various output media available these conditions may or may not cause poor legibility in the hardcopy output you receive.**

**If this block is checked, the copy furnished to DRDCIM contained pages with colour printing, that when reproduced in Black and White, may change detail of the original copy.**

# **Investigation of Crack Turning in Fracture in Ship Structures**

D.R. Smith  
Suite 707  
5959 Spring Garden Road,  
Halifax, Nova Scotia

Contract No. W7707-0-8234/001/HAL

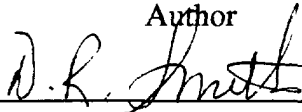
**Defence Research Establishment Atlantic**

Contractor Report

DREA CR 2001-067

July 2001

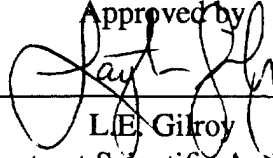
Author



---

D.R. Smith

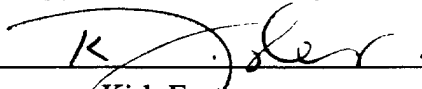
Approved by



---

L.E. Gilroy  
Contract Scientific Authority

Approved for release by



---

Kirk Foster  
Chair/Document Review Panel

The scientific or technical validity of this Contract Report is entirely the responsibility of the contractor and the contents do not necessarily have the approval or endorsement of Defence R&D Canada.

© Her Majesty the Queen as represented by the Minister of National Defence, 2001

© Sa majesté la reine, représentée par le ministre de la Défense nationale, 2001

## Abstract

---

The ability to predict crack propagation in a ship structure by finite element analysis based on linear elastic fracture mechanics was investigated. The investigation showed that the stress intensity factor at the crack tip, the number of cycles of constant amplitude loading to reach the critical intensity factor, and the critical length of the crack could be accurately predicted. The investigation concentrated on the ability to predict crack turning during propagation. Cracks originating at a plate edge, at a hole, and in the centre of a plate were evaluated. The results showed that crack turning was most likely to occur under mixed mode loading combining shear and tension.

## Résumé

---

La capacité de prévoir la propagation des fissures dans la structure d'un navire à l'aide de l'analyse par éléments finis basée la mécanique de rupture élastique linéaire a été étudiée. L'étude a montré que le facteur d'intensité des contraintes à la pointe de la fissure, le nombre de cycles de mise en charge à amplitude constante requis pour atteindre le facteur d'intensité critique et la longueur critique de la fissure pouvaient être prévus avec précision. L'étude était axée sur la capacité de prévoir le changement de direction de la fissure au cours de sa propagation. Les fissures émanant du bord d'une tôle, d'un trou ou du centre d'une tôle ont été évaluées. Les résultats ont montré que le changement de direction de la fissure risquait surtout de se produire en conditions de mise en charge en mode mixte combinant cisaillement et tension.

This page intentionally left blank.

## Executive summary

---

### Introduction

Catastrophic structural failure of ship structures have been shown to be caused by rapid growth of a crack in their plating. For this reason considerable attention is paid to any crack found in a ship's primary structure during inspection. Methods have been developed to predict the rate of crack growth based on linear elastic fracture mechanics (LEFM). It has been shown by these methods that, when the stress intensity at the tip of a crack in a plate due to a loading condition reaches a critical stress intensity factors ( $K_{Ic}$ ), the crack will propagate as if the hull material is brittle material, in some cases propagating at the speed of sound. The  $K_{Ic}$  value is obtained for different materials by laboratory testing of cracked plates subjected to constant amplitude loading. With these  $K_{Ic}$  values available, a structures analyst can determine the number of load cycles an identified crack will survive before it begins to rapidly propagate. The length of the crack on reaching  $K_{Ic}$  can also be predicted. A finite element analysis approach for LEFM is being developed for the Defense Research Establishment Atlantic (DREA) to make these predictions. Using the finite element method, the ship structure in the region of the crack is modeled with finite elements and special crack tip elements are used at the crack tip to predict the stress intensity factor. With these tools, assessments can be made as to whether a discovered crack is likely to present a problem requiring immediate repair or that its growth is such that it will not be a problem until a convenient repair opportunity. The predicted results of course would be confirmed by regular inspections.

### Principal Results

An investigation of the ability of the DREA LEFM software to predict crack growth to failure was carried out with special attention applied to its ability to predict turning of the crack as it propagates. The knowledge of how a crack is likely to turn as it grows is important as it can be used in deciding on the effect of the location of holes and other stress concentrators factors in a structure. The investigation showed that the VAST crack element performed well and that the software predicted stress intensity factors and the amount of crack growth with good accuracy. Crack turning was shown not to occur under pure tension loads (known as Mode I loads). Under pure shear loads (known as Mode II loads), a horizontal crack was shown to turn abruptly through an angle of 81 degrees. Under a combination of Mode I and Mode II loads there was pronounced turning in an edge cracked plate with and without the presence of a hole. The investigation also looked at the propagation of a crack from a stress concentration at a hole under mixed mode loading. In this case the crack

turned only at the extreme end of its growth as it approached  $K_{Ic}$ . The growth of a crack in a bulkhead model was shown to propagate to a hole without turning and without reaching the stress intensity factor that would indicate brittle fracture.

## **Significance of Results**

The investigation showed the current DREA LEFM software can predict crack turning during propagation. The software has the potential of becoming a powerful tool for assessing whether a detected crack in a critical region of a ship structure could become a serious problem with regard to ship safety. The use of the current software is limited to simple geometries. It should be developed to handle more complex structures which include fillet welds and reinforcing around openings. Because most ship hull loads are of variable amplitude, the ability to handle this type of loading should be added to the current constant amplitude capability.

D.R. Smith; 2001; Investigation of Crack Turning in Fracture in Ship Structures; DREA CR 2001-067; Defence Research Establishment Atlantic.

# Sommaire

---

## Introduction

On a observé que la rupture structurale catastrophique des structures d'un navire était causée par la propagation rapide d'une fissure dans le bordé. C'est pourquoi on accorde une attention considérable à toute fissure observée dans la structure primaire d'un navire lors de l'inspection. Des méthodes basées sur la mécanique de rupture élastique linéaire (MREL) ont été élaborées pour prévoir la vitesse de propagation des fissures. Elles ont montré que, lorsque l'intensité des contraintes à la pointe d'une fissure dans une tôle résultant d'une mise en charge atteint un facteur d'intensité des contraintes critique ( $K_{Ic}$ ), la fissure se propage comme si le matériau de la coque était un matériau fragile, dans certains cas à la vitesse du son. La valeur de  $K_{Ic}$  est obtenue pour différents matériaux par des essais en laboratoire effectués sur différentes tôles fissurées mises en charge à amplitude constante. Avec ces valeurs de  $K_{Ic}$  disponibles, un analyste des structures peut déterminer le nombre de cycles de mise en charge que peut supporter une fissure identifiée avant de commencer à se propager rapidement. La longueur de la fissure lorsque la valeur de  $K_{Ic}$  est atteinte peut aussi être prévue. Une méthode d'analyse par éléments finis pour la MREL est actuellement élaborée pour le Centre de recherches pour la défense Atlantique (CRDA) en vue de faire ces prévisions. On utilise la méthode par éléments finis pour modéliser la structure du navire dans la région de la fissure et on utilise des éléments de pointe de fissure particuliers pour prévoir le facteur d'intensité des contraintes. Avec ces outils, on peut déterminer si une fissure observée risque de poser un problème nécessitant une réparation immédiate ou si sa vitesse de propagation est tellement faible qu'elle ne posera pas de problème pendant la durée de vie du navire. Les résultats seraient évidemment confirmés par des inspections régulières.

## Principaux résultats

On a effectué une étude portant sur le logiciel de MREL du CRDA en vue de déterminer sa capacité de prévoir la transformation d'une fissure en rupture, en portant une attention particulière à sa capacité de prévoir le changement de direction de la fissure au cours de sa propagation. Il est important de savoir comment une fissure risque de changer de direction au cours de sa propagation, car cette information peut être utilisée pour déterminer l'incidence de l'emplacement des trous et d'autres éléments de concentrations des contraintes dans une structure. L'étude a montré que l'élément de fissure avait un bon comportement et que le logiciel permettait de prévoir avec une bonne précision le degré de propagation de la fissure. On a observé que le changement de direction de la fissure ne se produisait

pas en présence de charges de tension pure (appelées charges de mode I). On a constaté qu'une fissure horizontale soumise à des charges de cisaillement pur (appelées charges de mode II) présentait un changement brusque de direction d'un angle de 81 degrés. Avec une combinaison de charges de mode I et de mode II, on a observé un changement de direction marqué dans une tôle comportant une fissure de bord, avec et sans trou. L'étude a aussi porté sur la propagation d'une fissure émanant d'un point de concentration des contraintes adjacent à un trou en mode mixte de mise en charge. Dans ce cas, la fissure n'a changé de direction qu'à l'extrémité de son trajet de propagation, au voisinage de  $K_{Ic}$ . On a observé qu'une fissure dans un modèle de cloison se propageait jusqu'à un trou sans changer de direction et sans atteindre le facteur d'intensité des contraintes qui indiquerait une rupture fragile.

## Signification des résultats

L'étude a montré que le logiciel actuel de MREL du CRDA permet de prévoir le changement de direction d'une fissure au cours de sa propagation. Ce logiciel pourrait devenir un outil puissant pour déterminer si une fissure détectée dans une région critique de la structure d'un navire risque de poser un problème grave sur le plan de la sécurité du navire. L'utilisation du logiciel actuel est limitée aux formes géométriques simples. Il faudrait perfectionner le logiciel pour qu'il puisse traiter des structures plus complexes comprenant des soudures d'angle et des éléments de renforcement autour d'ouvertures. Comme la plupart des charges exercées sur les coques des navires sont d'amplitude variable, on devrait ajouter la capacité de traitement de ce type de charges à la capacité de traitement actuelle des charges d'amplitude constante.

D.R. Smith; 2001; Investigation of Crack Turning in Fracture in Ship Structures; DREA CR 2001-067; Centre pour la Recherche de la Défense Atlantique.

## Table of contents

---

Abstract . . . . .	i
Résumé . . . . .	i
Executive summary . . . . .	iii
Sommaire . . . . .	v
Table of contents . . . . .	vii
List of figures . . . . .	viii
1 Introduction . . . . .	1
2 Crack Initiation . . . . .	2
3 Stress Intensity Factors . . . . .	3
4 Crack Propagation . . . . .	5
4.1 Crack Propagation Under Mode I Loading . . . . .	9
4.2 Crack Propagation Under Mode II Loading . . . . .	11
5 Crack Turning During Propagation . . . . .	11
5.1 Crack Turning During Propagation Under Mixed Mode Loading . . . . .	14
5.2 Crack Turning in the Presence of a Hole and Mode I Loading . . . . .	16
5.3 Crack Turning in the Presence of a Hole With Edge Shear . . . . .	18
5.4 Crack Turning in Presence of a Hole Under Combined Shear and Compression . . . . .	22
6 Propagation of a Crack Originating at a Hole . . . . .	22
7 Crack Propagation and Turning in a Ship Structural Detail . . . . .	26
8 Discussion . . . . .	31
References . . . . .	32

## List of figures

---

1	The Opening and Shearing Modes of Loading for Crack Surface Displacements . . . . .	2
2	Crack Initiation Model Subjected to a Uniform Constant Amplitude Tension Load . . . . .	3
3	S-N Curve of Stress Versus Cycles to Failure . . . . .	4
4	A Single Edge Cracked Plate of Width $W$ and Crack Length $a$ . . . . .	5
5	A Comparison of Calculated Stress Intensity Factors With Those Obtained Using the Crack Element in VAST for the Model Shown in Figure 4 . . . . .	6
6	Stress Intensity Factor Versus the Number of Elements Beyond the Crack Tip . . . . .	6
7	Crack Propagation Regions . . . . .	7
8	Effect of Initial Flaw Size on Number of Cycles . . . . .	8
9	$R = -1$ Constant Amplitude Loading . . . . .	8
10	$R = 0$ Constant Amplitude Loading . . . . .	9
11	Finite Element Plate Model with a Starting Crack Length of 5 mm . . . . .	10
12	Correction Factor $f(\frac{a}{W})$ for Estimating Critical Crack Length . . . . .	11
13	Finite Element Plate Model Showing Crack Growth of 70 mm . . . . .	12
14	Fatigue Crack Growth Rate . . . . .	12
15	Fatigue Crack Growth to $K_{Ic} = 5200$ . . . . .	13
16	Centrally Cracked Plate Under Mode II Loading Showing a Turn of 81 Degrees During the First Increment of Crack Growth . . . . .	13
17	Finite Element Model of Inclined Crack . . . . .	14
18	Stress and Propagation of the Crack . . . . .	15

19	Edge Shear Loading on Crack Turning Model with an Initial Crack of 10 mm . . . . .	15
20	Stress Intensity Factor and Crack Propagation to Fracture Under an Edge Shear Loading . . . . .	16
21	Mode I loading of Plate Model with Hole . . . . .	17
22	Stress Distribution in the Plate Model with a Hole, Under Mode I Loading . . . . .	17
23	Crack Turning in the Plate Model with a Hole Under Mode I Loading .	18
24	Crack Propagation with the Initiating 10 mm Crack at the Top Edge . .	19
25	The Propagation to Failure of the Crack in the Top Edge of the Plate with the Hole Under Mode I Loading . . . . .	19
26	Loading on Crack Turning Model with Hole and an Initial Crack of 10 mm . . . . .	20
27	Stress Intensity Factor and Crack Propagation to Fracture for the Crack Turning Model with Hole . . . . .	20
28	Comparison of Crack Turning with and without the Presence of a Hole	21
29	Loading on the Crack Turning Model with the Hole Closer to the Bottom Edge with an Initial Crack of 10 mm . . . . .	21
30	Stress Intensity Factors and Crack Propagation to Fracture for the Model with the Hole Closer to the Bottom Edge . . . . .	22
31	The Initial Crack and Mixed Mode Loading of the Plate with a Hole . .	23
32	Crack Propagation and Stress Intensity Factors for Mixed Mode Loading Fracture . . . . .	23
33	Stresses in the Plate with a Hole Without the Crack . . . . .	24
34	Crack Propagation from the Stress Concentration at the Hole . . . . .	24
35	Crack Growth Rate to Failure for a Crack Originating at a Hole . . . .	25
36	Finite Element Model of a Longitudinal Bulkhead Detail . . . . .	26

37	The MAESTRO Finite Element Model of a Ship from Which the Longitudinal Bulkhead Detail was Taken . . . . .	27
38	Maximum Constant Amplitude Stress Distribution in the Longitudinal Bulkhead Detail . . . . .	27
39	Local Portion with the Starting Crack Extracted from the Longitudinal Bulkhead Detail . . . . .	28
40	The Boundary Conditions Automatically Applied to the Boundaries Between the Local and Global Models . . . . .	29
41	Propagation of the Crack in the Longitudinal Bulkhead . . . . .	29
42	Growth of the Crack in the Longitudinal Bulkhead . . . . .	30

# 1 Introduction

---

The failure of a ship structure due to a rapid propagation of a critically located crack is a well known phenomenon. The failure process begins with fatigue crack initiation at a stress concentration under cyclic loading conditions. This is followed by the propagation of the crack to a point where a possible ultimate or brittle fracture may occur which could result in as serious a failure as the ship breaking in two. The main factors which govern the susceptibility of a structure to fracture are material toughness, crack size, and stress. The fracture toughness is measured by the critical stress intensity factor  $K_{Ic}$ . It has been shown that when the stress at the crack tip reaches this value there is a rapid increase in crack growth which can lead to fracture. When the stress intensity at the crack tip is below a threshold value  $K_{th}$  the crack will not grow under cyclic load. In between these two extreme values, test data plotted for various types of metals has shown the crack will grow at a rate of the Paris-Erdogan[1] equation

$$\frac{da}{dN} = C(\Delta K)^m$$

where

$a$  = instantaneous crack length

$N$  = number of cycles

$C$  = intercept of log/log plot  $\frac{da}{dN}$  versus  $\Delta K$

$\Delta K$  = stress intensity factor range  $K_{max} - K_{min}$

$m$  = slope of log/log plot  $\frac{da}{dN}$  versus  $\Delta K$

The line of a crack may turn as it propagates as a result of loading or geometry effects. The turning should be accounted for in the fracture analysis as it will affect the time to failure as it may increase or shorten the crack length.

Crack initiation and crack propagation in a structure can be predicted by finite element methods through the use of a finite element program such as VAST[2] which has a crack tip element in its library of elements for calculating stress intensity factors. The structure including the crack, can be modeled using the finite element modeling program MG/DSA[3]. The calculated stress intensity factors are then used along with the stress range and material properties, such as stress versus cycles to failure (S-N curves) and  $C$  and  $m$  values, to obtain a fatigue assessment of the structure using a program such as LIFE3D[4].

This report covers the determination of crack initiation, crack propagation, and the turning of the crack as it propagates under the opening and shearing modes of loading and the crack surface displacements known as Mode I and Mode II as shown in

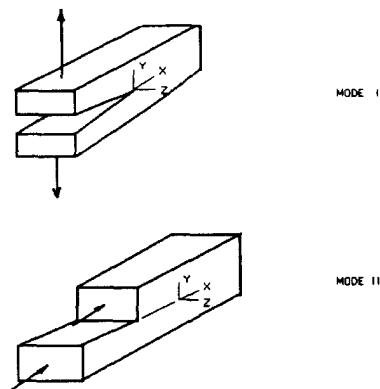


**Figure 1:** *The Opening and Shearing Modes of Loading for Crack Surface Displacements*

Figure 1. A variety of geometries were examined using finite element methods and the fatigue assessment program LIFE3D.

## 2 Crack Initiation

Crack initiation prediction is based on the identification of notches and flaws, typically found in a structure, for which a stress concentration factor can be assumed. Under a cyclic load, very small cracks will form at a stress concentration after a small percentage of the total cycles to complete fracture. A crack initiation analysis is therefore an attempt to predict the number of cycles of loading required to cause a crack to form for which a crack propagation analysis can be carried out.

A simple finite element model of a plate, under a constant amplitude tension load, was used to demonstrate a crack initiation analysis. The model is shown in Figure 2. The location of a stress concentration is identified by a crack line along which the crack is expected to progress. The flaw was modeled by selecting a stress concentration factor for a notch at the point identified by the crack. A large notch radius approaching a straight line has a stress concentration[5] approaching 1 while a very small radius can have a stress concentration factor approaching 3. The additional data required for the program to estimate the number of cycles of constant amplitude cyclic loading to initiate a crack can be obtained by referring to the S-N curve for the material used. A typical S-N curve is shown in Figure 3 from which the required following data can be extracted.

Material 5 mm Steel Plate

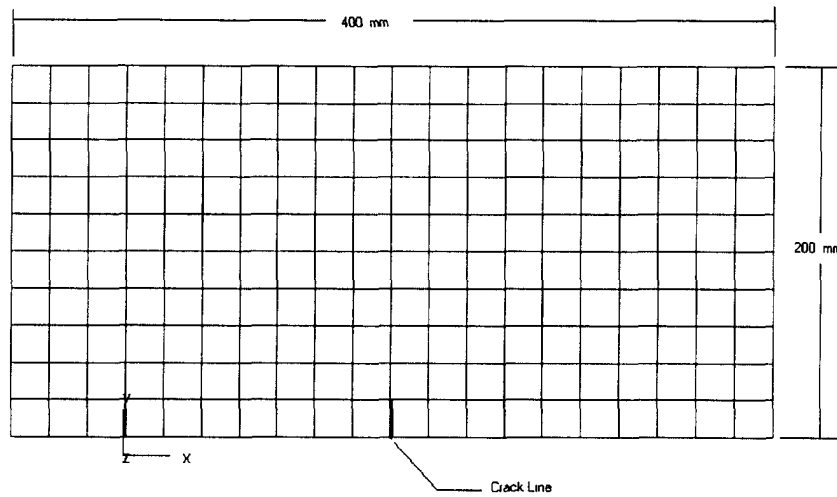


**Figure 2:** Crack Initiation Model Subjected to a Uniform Constant Amplitude Tension Load

- maximum stress of the S-N curve
- number of cycles at maximum stress
- slope of the S-N curve
- threshold stress for infinite life
- ultimate strength of the material

Three analyses, using the same constant amplitude load, were conducted to show the effect of the choice of stress concentration on the the number of cycles in the initiation phase. The results are shown in Table 1.

**Table 1:** The Number of Cycles Required for Crack Initiation

Stress Concentration Factor	Cycles to Cause Crack
1	1810
2	112
3	1.16

### 3 Stress Intensity Factors

The crack initiation stage of fatigue analysis is often regarded as unnecessary[6][7] in welded structures typically found in ships because of the presence of stress raisers

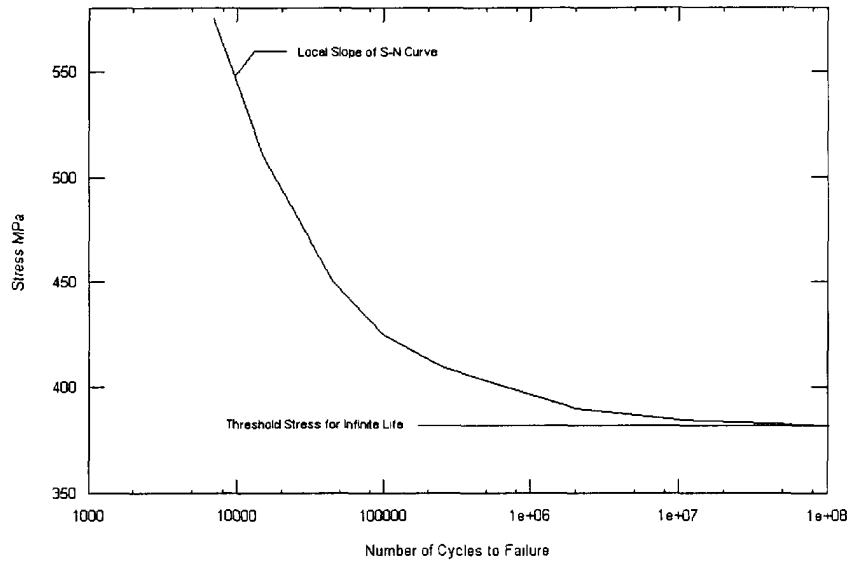


**Figure 3:** S-N Curve of Stress Versus Cycles to Failure

due to welds and other fabrication processes. The structures are assumed to be already cracked with small cracks of a size that equals or exceeds that which can be detected by the capability of the inspection process. If too small a crack length is chosen, it may not obey the principles of linear fracture mechanics.

The stress intensity factor  $K_I$  plays a major part in determining the crack growth per cycle  $da/dN$ . For a single edge crack in a plate, as shown Figure 4, the stress intensity factor can be determined with the following expression[7] with an accuracy within 0.5 % for a crack length to plate width ratios  $\frac{a}{W}$  less than 0.5.

$$K_I = \sigma_0 \sqrt{\pi a} f\left(\frac{a}{W}\right)$$

where

$K_I$  = stress intensity factor

$\sigma_0$  = uniform tensile stress

$a$  = crack length

$W$  = width of plate

$$f\left(\frac{a}{W}\right) = 1.12 - 0.231\left(\frac{a}{W}\right) + 10.55\left(\frac{a}{W}\right)^2 - 21.72\left(\frac{a}{W}\right)^3 + 30.39\left(\frac{a}{W}\right)^4$$

Stress intensity factors for the single cracked plate shown in Figure 4 were calculated for different crack lengths, using the above expression. These factors are

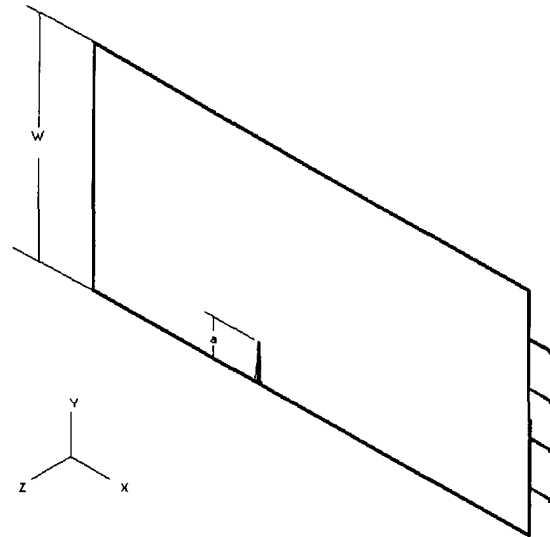


**Figure 4:** A Single Edge Cracked Plate of Width  $W$  and Crack Length  $a$

compared in Figure 5 with results obtained from a finite element model of the plate using the finite element program VAST and its 4-node crack element. The plate had a width of 200 mm. A tension load was applied to produce a uniform stress of 200 MPa in the 5 mm thick plate. There was excellent agreement between the VAST crack element stress intensity factors and the calculated values.

When conducting a finite element analysis to determine the stress intensity factor, it is necessary to choose the number of crack elements beyond and surrounding the crack tip. One four-node crack element beyond the tip is not sufficient. Figure 6 is a plot of stress intensity factor versus the number of elements beyond the crack. Five to six elements are required to produce satisfactory results. Five was the number used to obtain the VAST results in Figure 5.

## 4 Crack Propagation

---

Fatigue crack propagation can be represented by the sigmoidal shaped curve shown in Figure 7. When the value of the stress intensity factor range  $\Delta K$  is below the threshold stress intensity factor range  $\Delta K_{th}$  the crack will not grow. The  $K_{th}$  can be determined with the following equations for steel for  $R = \frac{\sigma_{min}}{\sigma_{max}}$  (stress ratio).

$$\Delta K_{th} = 190 \text{ MPa} \sqrt{\text{mm}} \quad \text{for } R < 0.1$$

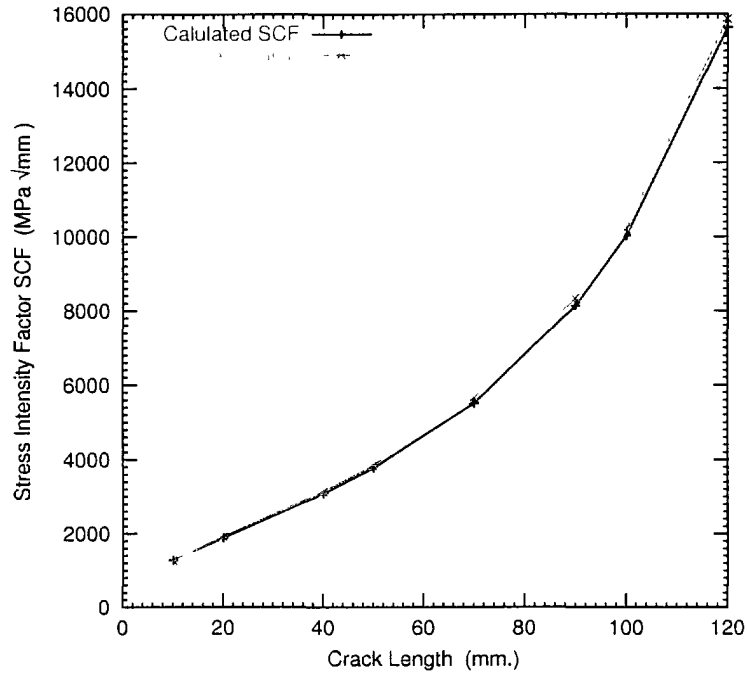


**Figure 5:** A Comparison of Calculated Stress Intensity Factors With Those Obtained Using the Crack Element in VAST for the Model Shown in Figure 4

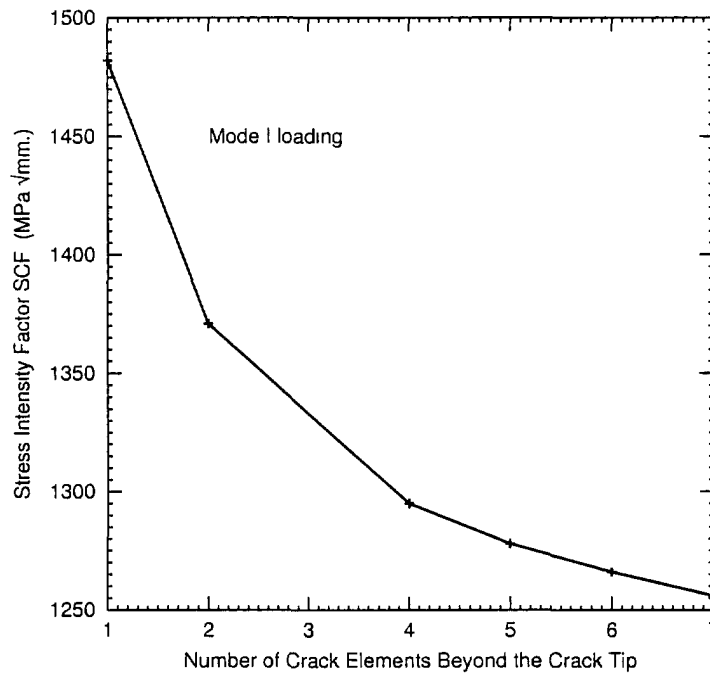


**Figure 6:** Stress Intensity Factor Versus the Number of Elements Beyond the Crack Tip

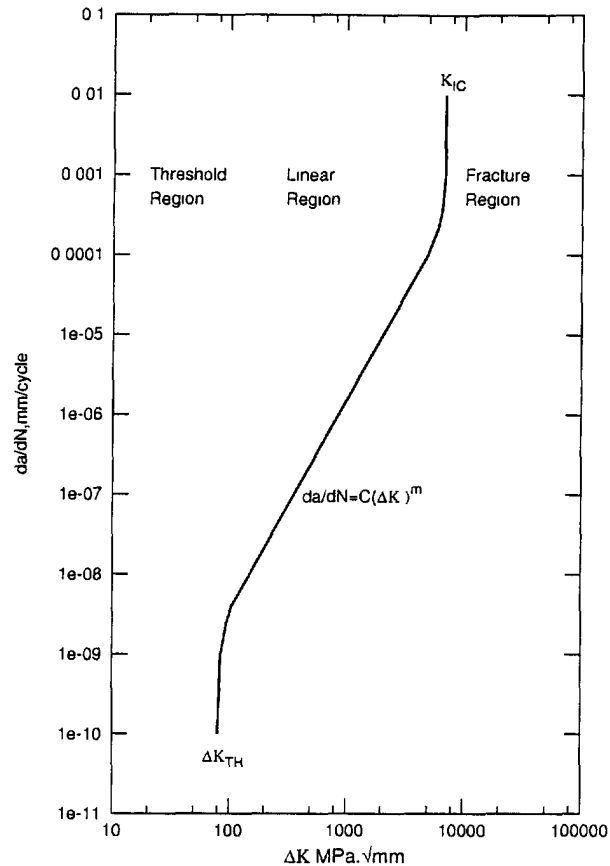


**Figure 7: Crack Propagation Regions**

$$\Delta K_{th} = 22(1 - 0.85)MPa\sqrt{mm} \quad \text{for } R \leq 0.1$$

The crack at the threshold region shows a rapid increase in crack growth at low  $K$  values followed by the region of the linear crack propagation growth as represented by the Paris equation. Finally the fracture region shows the accelerated growth to failure when the stress intensity factor approaches  $K_{Ic}$ . It is also important to note that the initial flaw size has an effect on the number of cycles to final fracture as can be seen in Figure 8.

The stress ratio  $R$ , resulting from a cyclic loading, affects the crack growth rate  $da/dN$  for a given  $\Delta K$ . An  $R$  value of  $-1$  indicates a full stress reversal as shown in Figure 9 and an  $R$  value of  $0$ , shown in Figure 10, is the load ratio used for Mode I fatigue testing of crack specimens and indicates that the stress cycles vary from  $\sigma_{min} = 0$  to  $\sigma_{max}$ .

Structural steels are only mildly affected by  $R$  in the intermediate crack growth

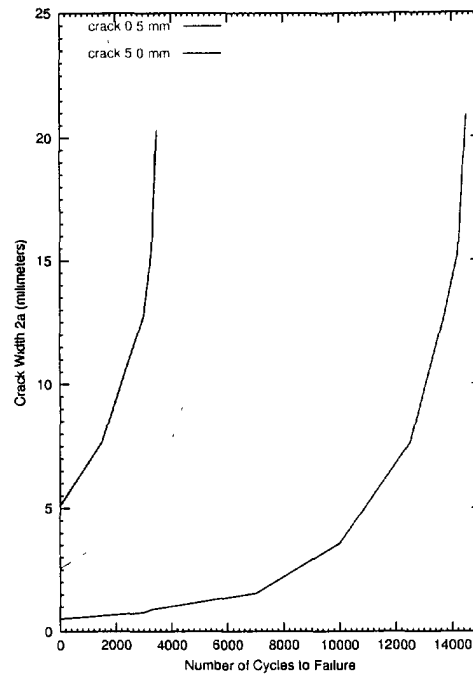


Figure 8: Effect of Initial Flaw Size on Number of Cycles

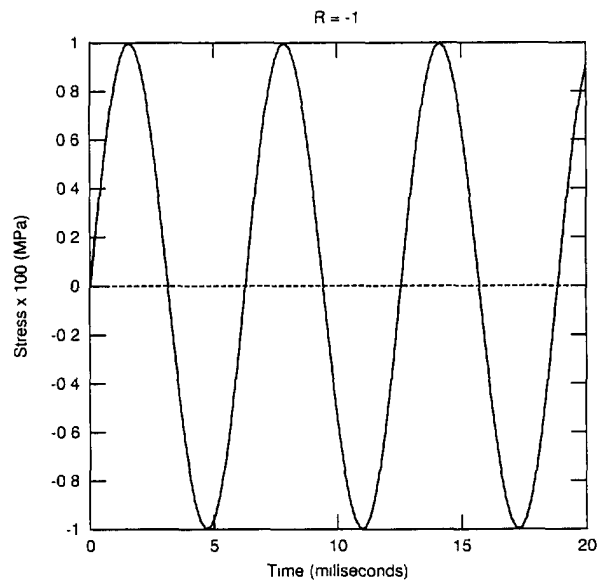
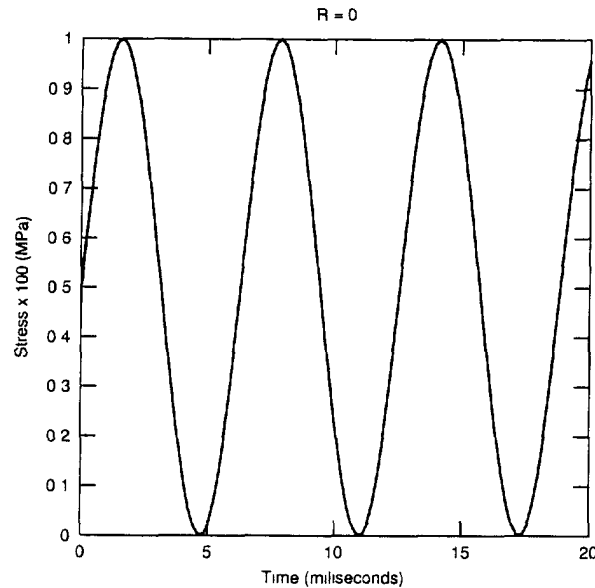


Figure 9:  $R = -1$  Constant Amplitude Loading



**Figure 10:  $R = 0$  Constant Amplitude Loading**

region. It has a more important effect at low growth rates and thus has an effect on the threshold value,  $\Delta K_{th}$ . Walker[8] has proposed a modification to the Paris-Erdogan equation for crack growth rate which includes the effect of  $R$ . It assumes however that for  $R < 0$  the compression part of the load cycle has no effect. This is not always the case as it has been shown that it can increase the crack growth rate in some steels by as much as 50%.

Another modification to the Paris-Erdogan equation to account for the effect of  $R$  has been proposed by Forman et al.[9]. It is also capable of predicting accelerated growth as the critical intensity factor  $K_{Ic}$  is approached.

#### 4.1 Crack Propagation Under Mode I Loading

A finite element analysis of crack propagation is generally carried out to predict two results. One is the number of load cycles to failure and the other is the length of the crack at failure. The number of cycles for incremental crack growth can be calculated with the following equation.

$$\Delta N = \frac{\Delta a}{C(1.12\sigma_r\sqrt{\pi a})^m}$$

This equation was applied to the  $W = 200\text{mm} \times 400\text{mm}$  plate shown in Figure 4 with a starting edge crack of  $a = 5 \text{ mm}$ . The 10 mm thick plate was loaded with a

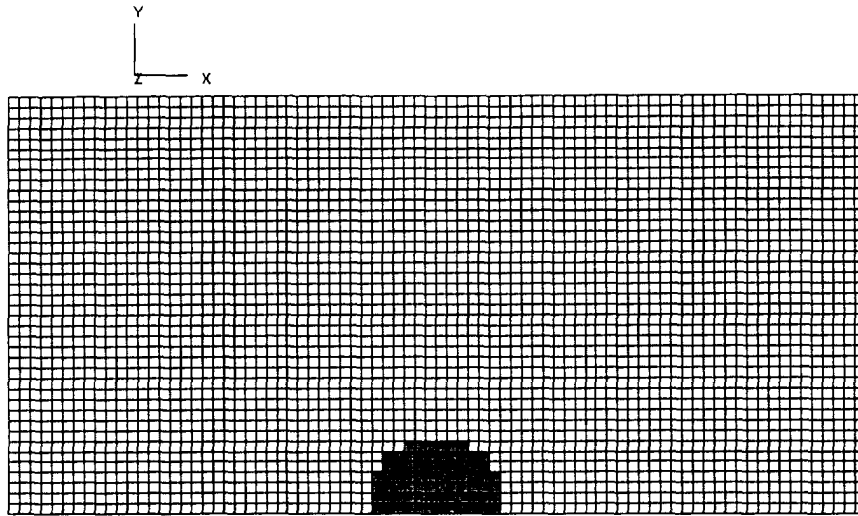


**Figure 11:** Finite Element Plate Model with a Starting Crack Length of 5 mm

uniform tension load to produce a constant amplitude stress of 200 MPa and stress range  $\sigma_r$  of 400 MPa for a  $R = -1$  loading case. An incremental crack growth of 5 mm was chosen. The plate was assumed to have the properties of A517 steel with a  $K_{Ic}$  of 5200, a  $C$  value of  $6.7 \times 10^{-11}$  and an  $m$  value of 2.26. The equation estimated the number of cycles for a crack growth of 5 mm to be 3392. The result obtained by finite element analysis using VAST and the auxiliary program K1K2CRACK[10] with the finite element model shown in Figure 11 gave the identical result of 3392 cycles. These results assume a constant value for the stress intensity factor over the crack growth of 5 mm. A better approach is to use the average crack length  $a_{avg}$  in the equation and to average the finite element results obtained for a 5 mm and a 10 mm crack. This procedure gives 2152 cycles for the equation and 2415 cycles for the finite element analysis.

The critical crack length can be predicted with the following equation.

$$a_{cr} = \frac{1}{\pi} \left( \frac{K_{Ic}}{f\left(\frac{a}{W}\right)\sigma_{max}} \right)^2$$

As described previously  $f\left(\frac{a}{W}\right)$  is a geometry factor dependent on the ratio of crack length to plate width. It is shown in Figure 12 plotted versus stress intensity factors for crack lengths from 5 mm to 100 mm at a  $\sigma_{max}$  of 200 MPa in the 200 mm wide plate model. At a  $K_{Ic}$  of 5200 the correction factor  $f\left(\frac{a}{W}\right)=1.78$ . These values, when applied to the above equation, predicted a critical crack length of 68 mm.

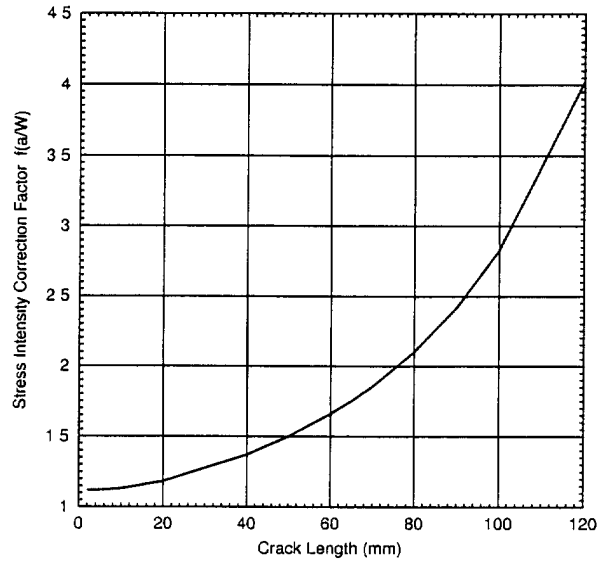


**Figure 12:** Correction Factor  $f\left(\frac{a}{W}\right)$  for Estimating Critical Crack Length

For comparison the number of cycles to produce a 68 mm crack, from an initial flaw of 5 mm in the plate, was predicted using the finite element model shown in Figure 13. Crack growth increments of 5 mm were used. The crack growth rate  $\frac{da}{dN}$  and stress intensity range  $\Delta K$  are plotted in Figure 14. The fatigue crack growth curve versus the number of loading cycles is shown plotted in Figure 15.

## 4.2 Crack Propagation Under Mode II Loading

Shear was applied to a center cracked plate as an example of Mode II loading, as shown in Figure 16. The crack turned through an angle of  $81^\circ$  in the first increment of growth. This is in good agreement with the angle obtained in a cracked plate under shear and a Poisson's ratio of .3 in reference [11].

## 5 Crack Turning During Propagation

Under a pure tension (Mode I) load, a crack will initiate and propagate in a straight line. If the crack is initially skewed such as in the model of the centre-cracked plate shown loaded in tension in Figure 17, its propagation can be determined by a step-by-step finite element analysis. For the model in the figure, the stress intensity factors were determined for the initial crack tip. The angle of the initial propagation was calculated using the program K1K2CRACK and a propagation increment of 10 mm. Using this angle, the finite element mesh was regenerated and the stress



**Figure 13: Finite Element Plate Model Showing Crack Growth of 70 mm**

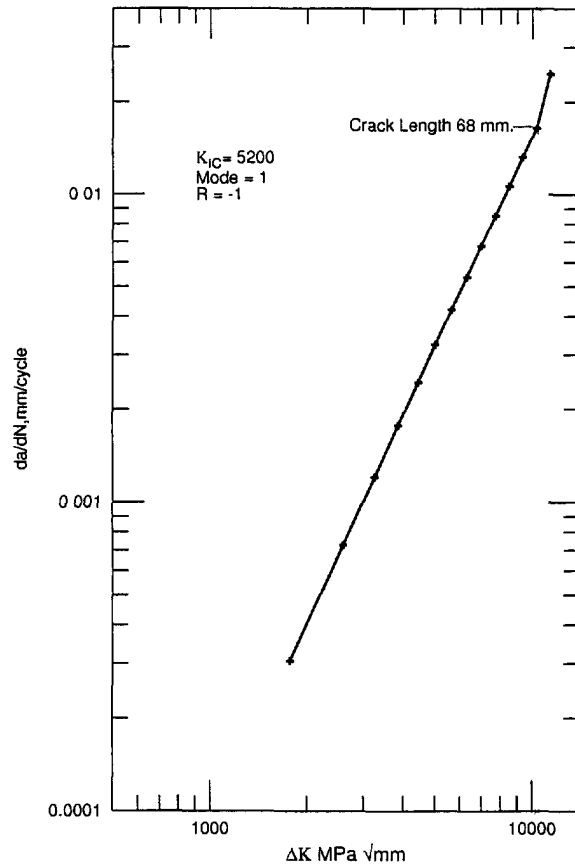


**Figure 14: Fatigue Crack Growth Rate**

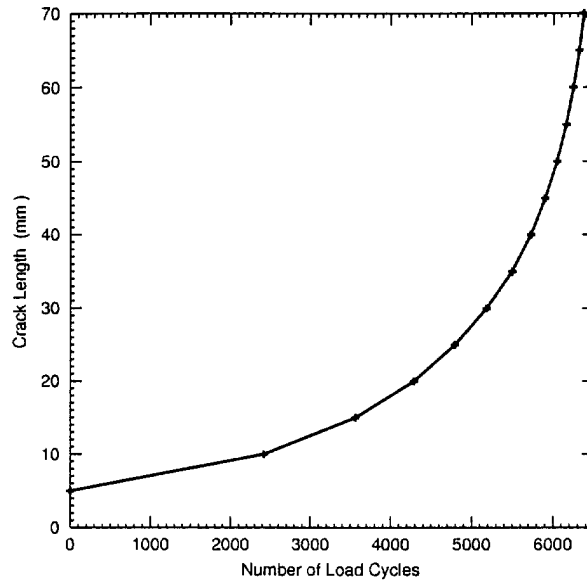


**Figure 15:** Fatigue Crack Growth to  $K_{Ic} = 5200$

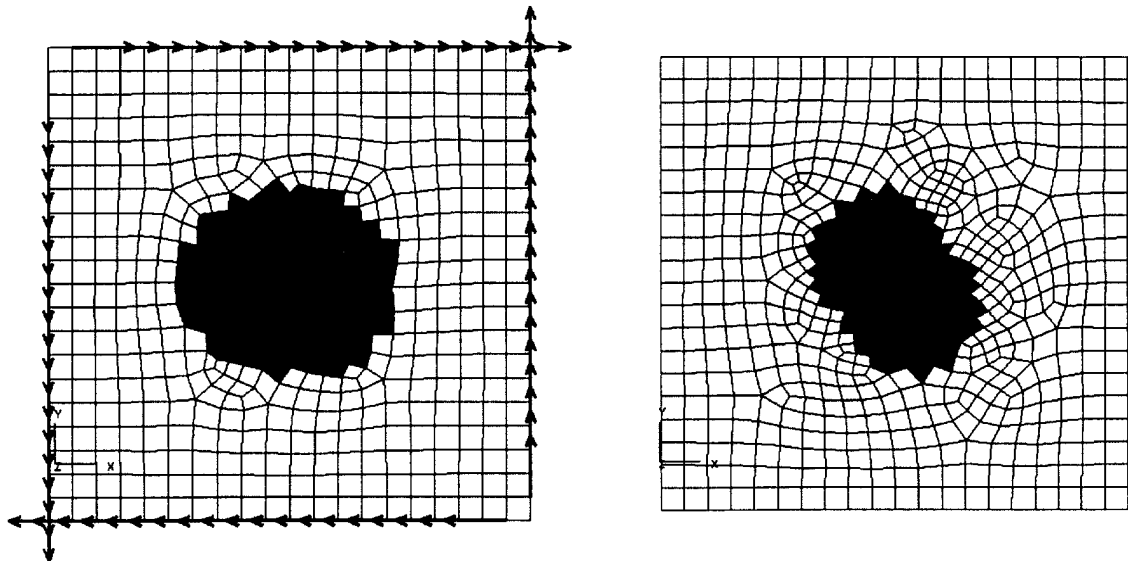


**Figure 16:** Centrally Cracked Plate Under Mode II Loading Showing a Turn of 81 Degrees During the First Increment of Crack Growth

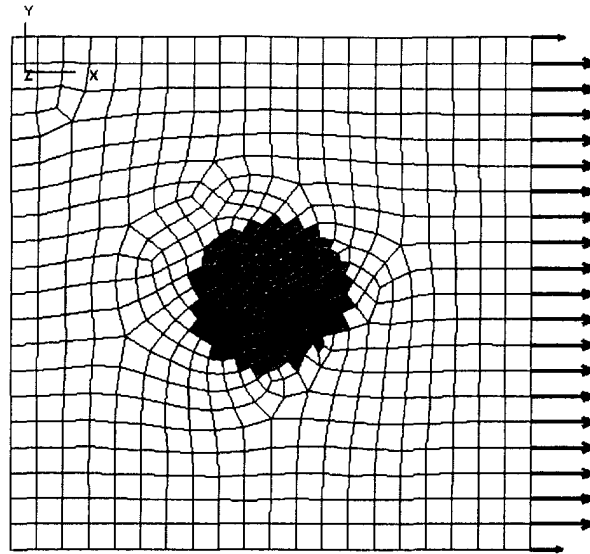


**Figure 17:** Finite Element Model of Inclined Crack

intensity factors determined for the new crack tip position. The process was continued until the stress intensity factors approached the  $K_{Ic}$  value of 5200. At this stage the path of the propagation had been fairly well established. There was an initial turning, from an angle of  $45^\circ$  degrees, through an angle of  $-49.09^\circ$  and then the crack propagated in a straight line as shown in Figure 18. The stress intensity factors for the upper and lower crack tips were essentially equal until the crack intensity factors approached the  $K_{Ic}$  value. The stress intensity factors at this point differed by 2 percent. The lower crack also showed a  $1^\circ$  turn from the straight line propagation.

## 5.1 Crack Turning During Propagation Under Mixed Mode Loading

Loads which generally occur in ship structures, are more likely to be mixed mode, thereby creating a combined stress situation. Under combined stress, the crack is likely to turn in a direction perpendicular to the maximum tangential stress at the crack tip. The edge cracked model shown in Figure 19 was subjected to a edge shear load which applied a combination of tension and shear to the crack tip. The step-by-step approach of remeshing the finite element model was used to determined stress intensity factors and the angle of propagation at the crack in 10 mm crack increments. The crack propagation to fracture is shown in Figure 20.

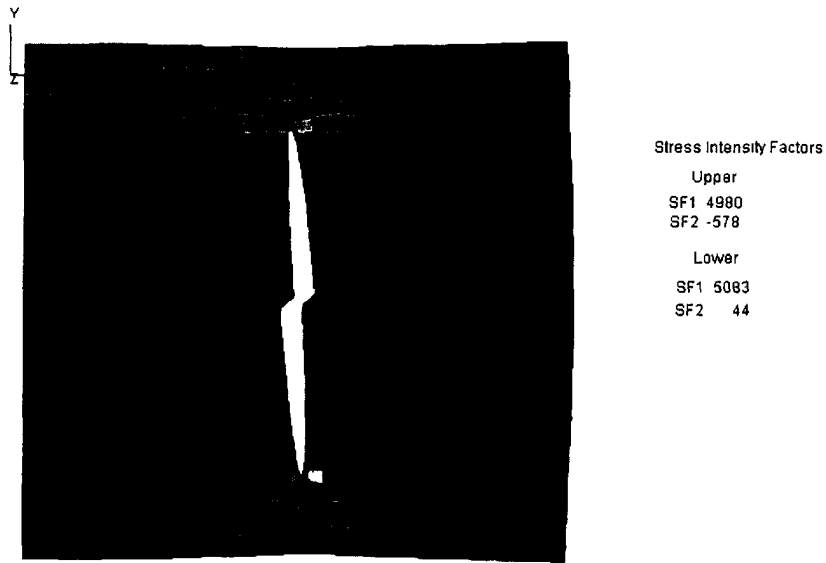


**Figure 18:** Stress and Propagation of the Crack

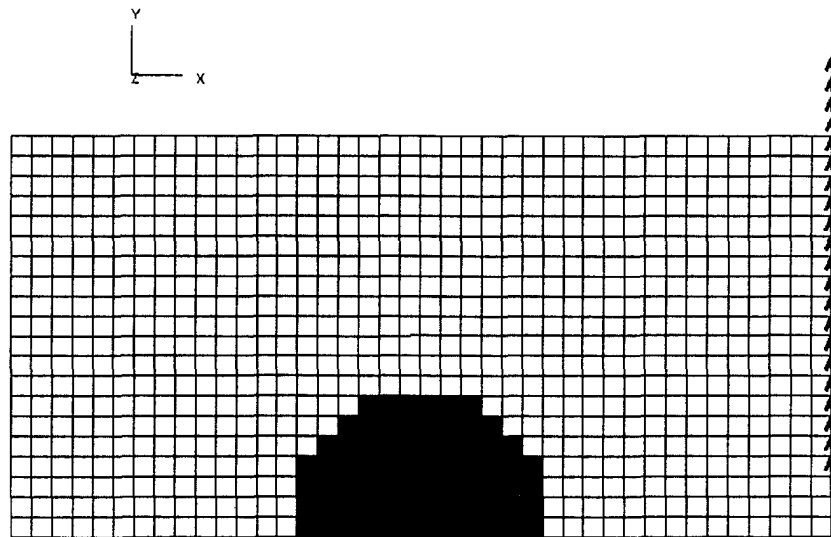


**Figure 19:** Edge Shear Loading on Crack Turning Model with an Initial Crack of 10 mm

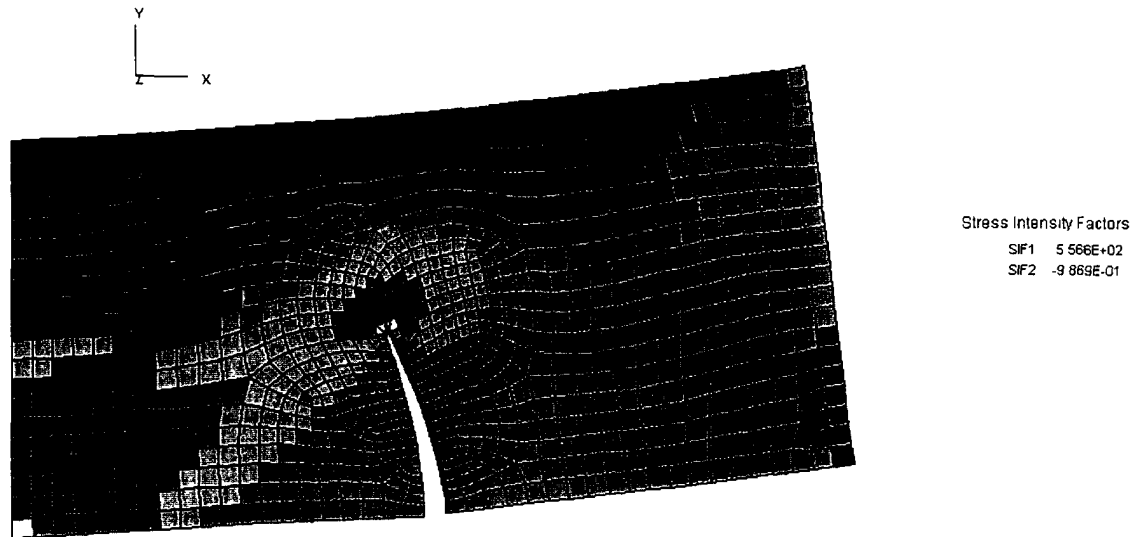


**Figure 20:** Stress Intensity Factor and Crack Propagation to Fracture Under an Edge Shear Loading

## 5.2 Crack Turning in the Presence of a Hole and Mode I Loading

Crack turning in the presence of a hole under the Mode I tension load shown in Figure 21 was examined. An initial crack of 10 mm crack was assumed to have formed at the lower edge of the model. Figure 22 shows the stress distribution in the model with the initiating crack. It is generally assumed that the crack will propagate on a trajectory perpendicular to the principal stress direction. On this basis, the initial crack location was chosen so that it would propagate to pass close to the hole and into the more complex stress field in its vicinity. As can be seen in Figure 23, the crack propagated in a straight line normal to the applied loads. As it approached the hole, it began to turn towards it, finally reaching and exceeding the critical stress intensity  $K_{Ic} = 5200$  indicating that the fracture was likely to include the hole. At a higher loading the crack would be shorter and fracture would take place before reaching the stress field at the hole and before any turning could occur.

The analysis was repeated with the crack located at the top edge of the model as shown in Figure 24. Starting from an initial straight crack length of 10 mm and assuming 10 mm increments of growth, it began its progression with a  $5^\circ$  turn away from the hole. The next increment of growth was at an additional angle of  $1.7^\circ$  degrees away from the hole. From there on, until fracture, the crack grew turning towards the hole exceeding the yield of 700 MPa prior to reaching the  $K_{Ic}$

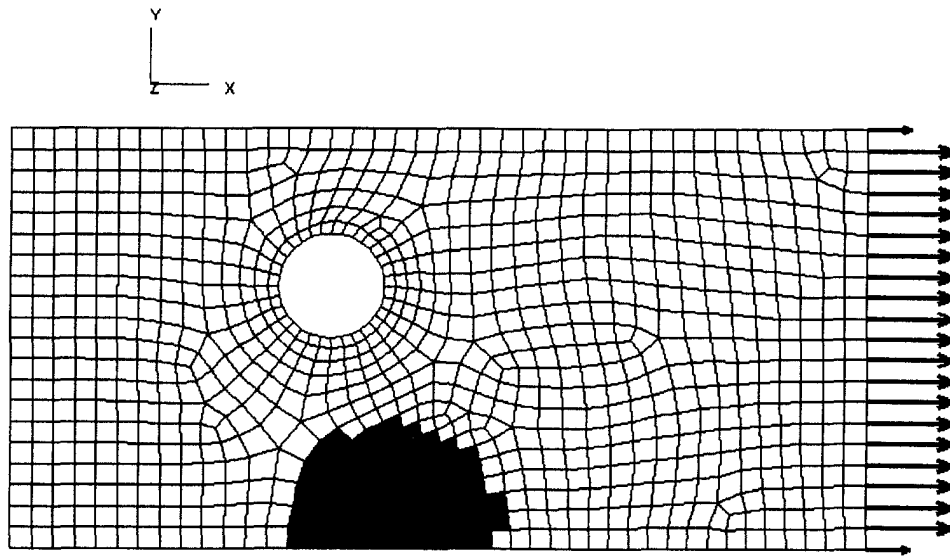


**Figure 21:** Mode I loading of Plate Model with Hole



**Figure 22:** Stress Distribution in the Plate Model with a Hole, Under Mode I Loading



*Figure 23: Crack Turning in the Plate Model with a Hole Under Mode I Loading*

value of 5200. The crack path at yield is shown in Figure 25.

### 5.3 Crack Turning in the Presence of a Hole With Edge Shear

The effect on crack turning of the presence of a hole in the model shown in Figure 19 was investigated. The same edge shear load was applied to the model (see Figure 26) and the step-by-step approach of remeshing after each crack extension was used. The resulting crack on reaching  $K_{Ic}$  is shown in Figure 27.

A comparison of the crack turning with and without the hole for the models in Figure 20 and Figure 27 is shown in Figure 28. The presence of the hole had little affect on the amount of turning when compared with the plate without the hole.

The affect of moving the hole closer to the initiating crack was investigated when under the edge shear load using the model shown in Figure 29. The results are shown in Figure 30. The angle at fracture for the closer hole was  $17.23^\circ$  at a length of 90 mm as compared to  $21.02^\circ$  and a length of 100 mm for the model with the more remote hole in Figure 27.

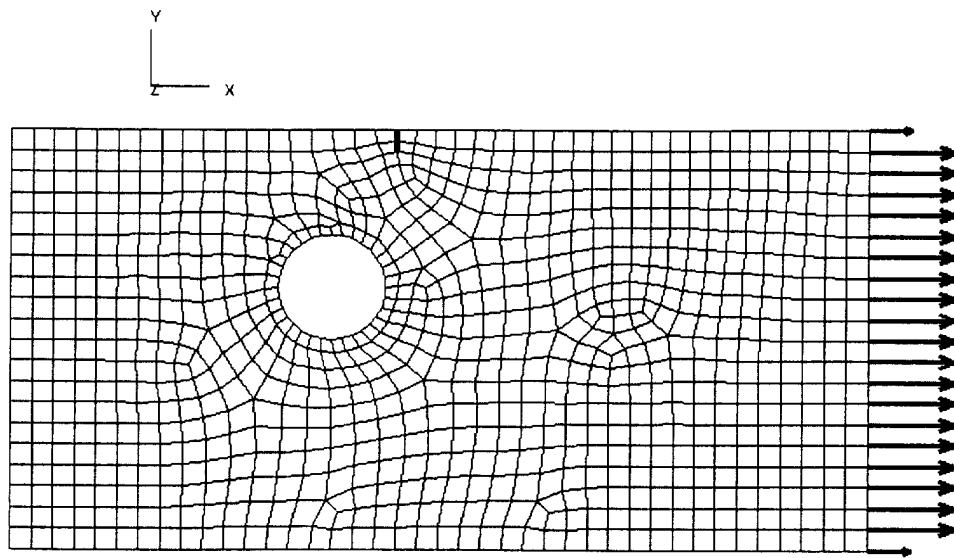


**Figure 24:** Crack Propagation with the Initiating 10 mm Crack at the Top Edge

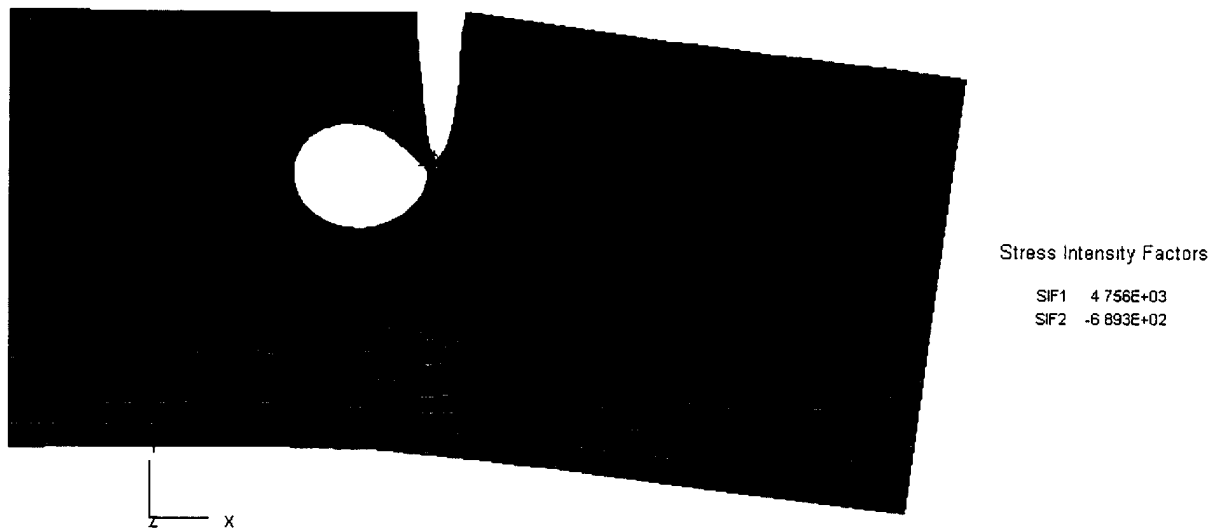


**Figure 25:** The Propagation to Failure of the Crack in the Top Edge of the Plate with the Hole Under Mode I Loading

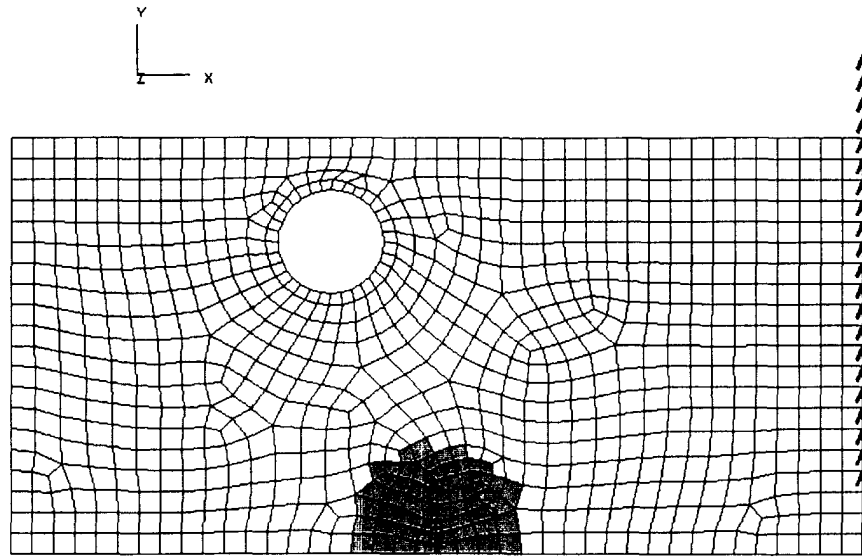


**Figure 26:** Loading on Crack Turning Model with Hole and an Initial Crack of 10 mm

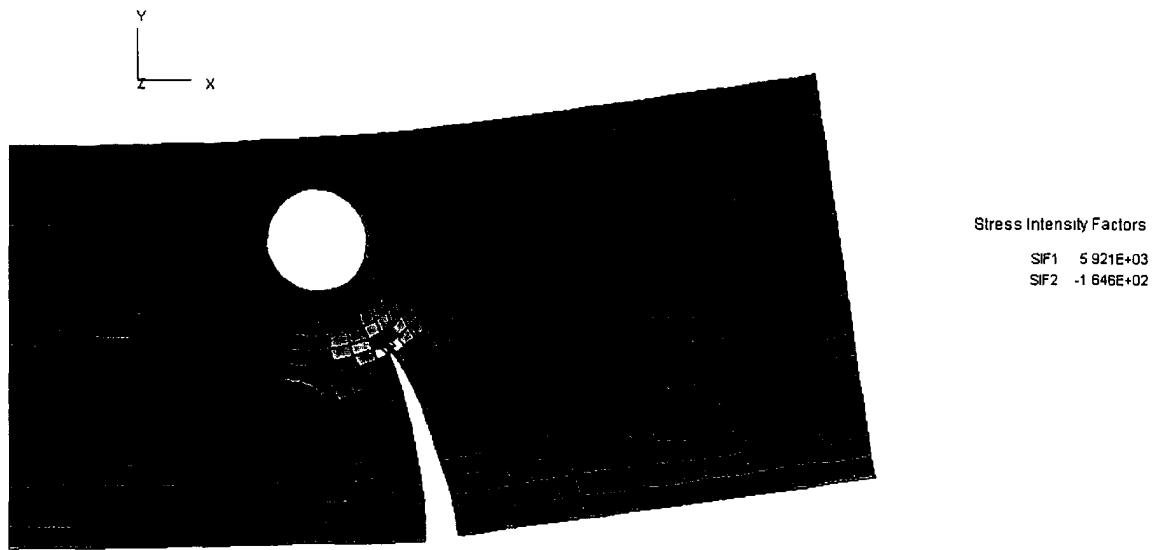


**Figure 27:** Stress Intensity Factor and Crack Propagation to Fracture for the Crack Turning Model with Hole

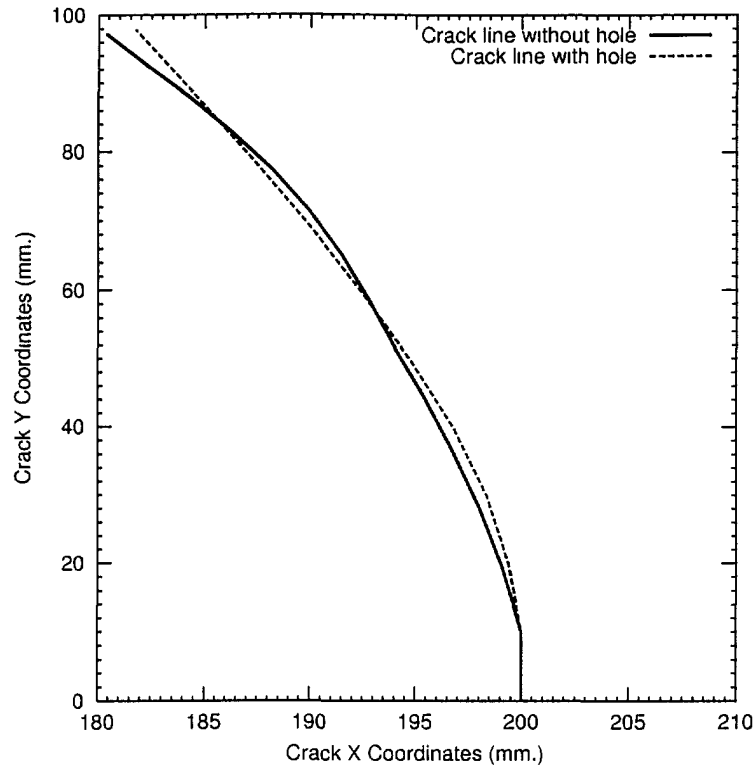


**Figure 28:** Comparison of Crack Turning with and without the Presence of a Hole

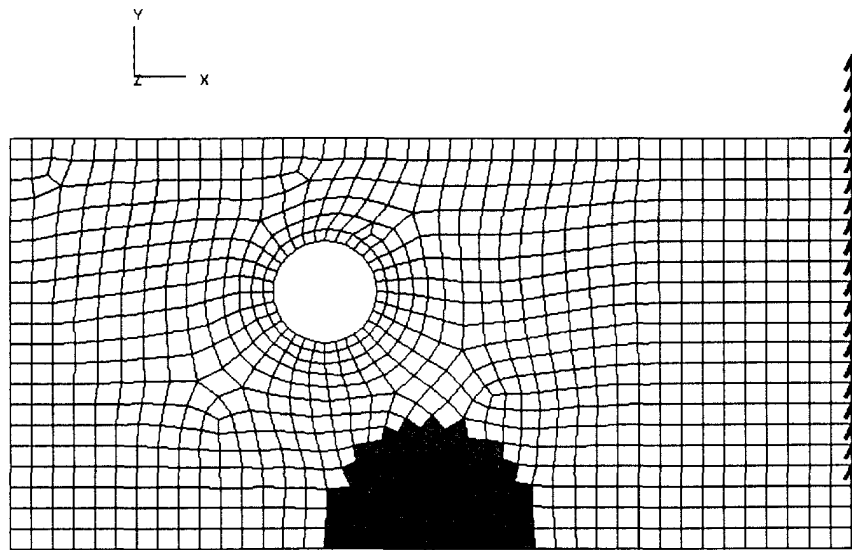


**Figure 29:** Loading on the Crack Turning Model with the Hole Closer to the Bottom Edge with an Initial Crack of 10 mm

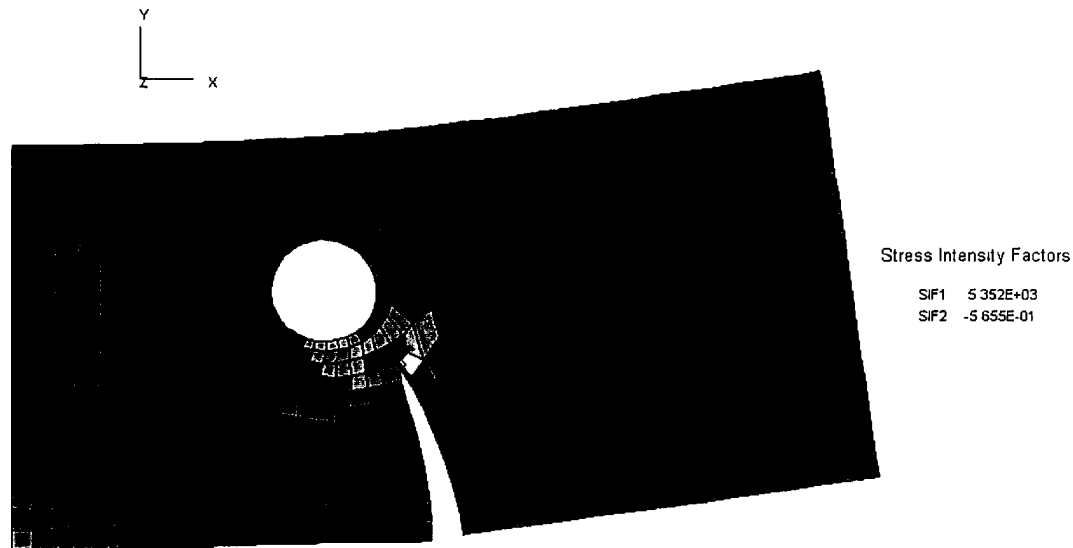


**Figure 30:** Stress Intensity Factors and Crack Propagation to Fracture for the Model with the Hole Closer to the Bottom Edge

## 5.4 Crack Turning in Presence of a Hole Under Combined Shear and Compression

The affect of adding a compression component to the edge shear load was examined. The loading is shown in Figure 31 and the resulting crack growth to fracture (100 mm) in Figure 32. The crack angle at fracture was  $25.64^\circ$  indicating much more turning than resulted under the edge shear alone.

## 6 Propagation of a Crack Originating at a Hole

---

The model shown in Figure 31, with the same mixed mode loading, was used to predict the growth of a crack when it originates at the stress concentration at the hole. The stresses due to the loading without the presence of the initiating crack are shown in Figure 33. The crack growth to a  $K_I$  of 5329 in the plate with a  $K_{Ic}$  of 5200 is shown in Figure 34. The crack growth rate during propagation is shown in Figure 35. The crack propagated in a straight line from the initiating point finally turning through an angle of  $4.7^\circ$  just prior to reaching the critical stress intensity factor of 5200 at a crack length of 45 mm. This was accompanied by the expected rapid increase in the crack growth rate.

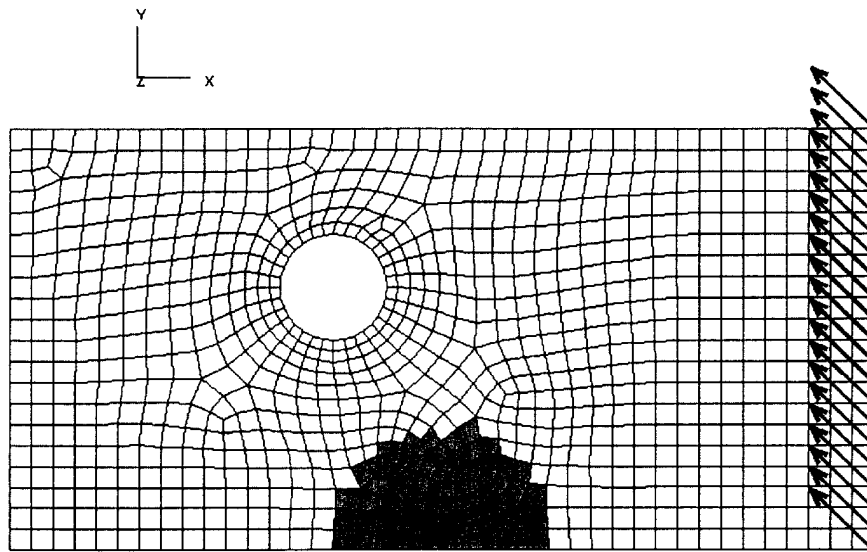


**Figure 31:** The Initial Crack and Mixed Mode Loading of the Plate with a Hole

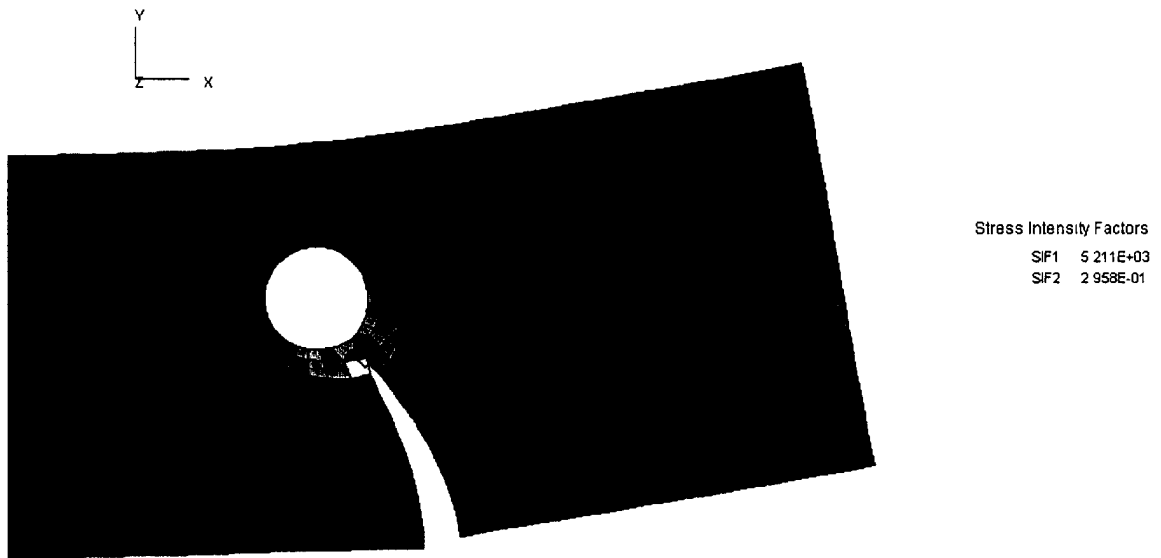


**Figure 32:** Crack Propagation and Stress Intensity Factors for Mixed Mode Loading Fracture

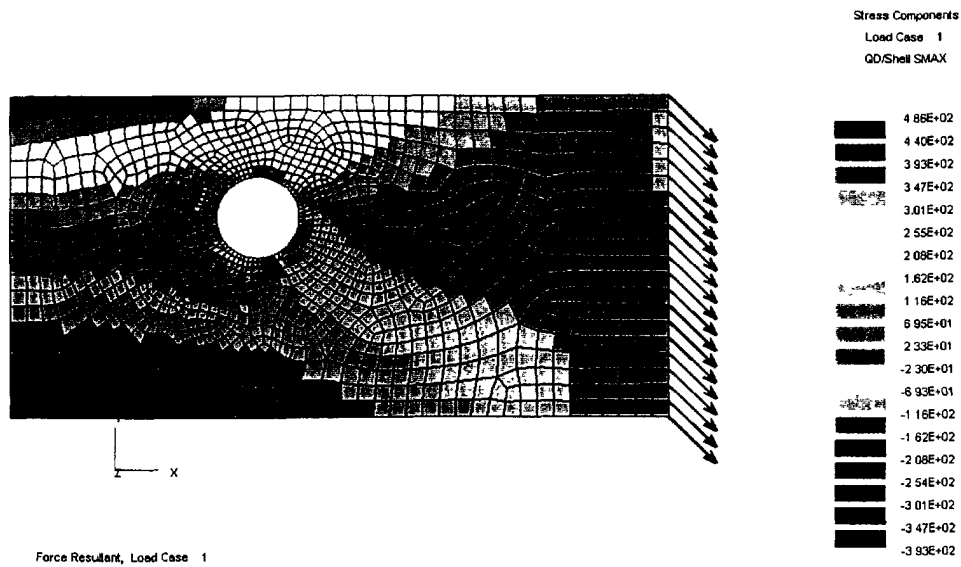


Figure 33: Stresses in the Plate with a Hole Without the Crack

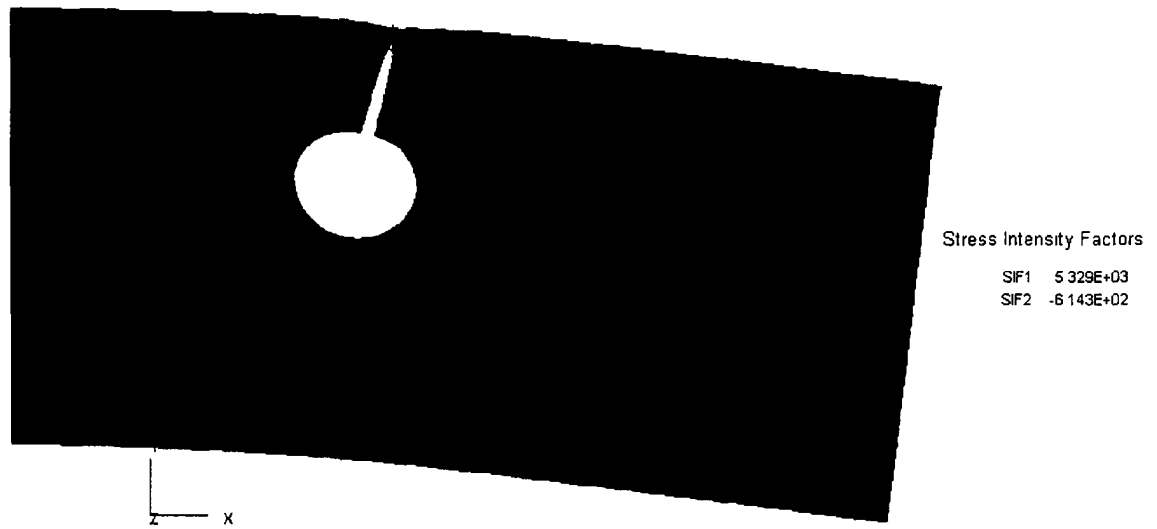


Figure 34: Crack Propagation from the Stress Concentration at the Hole

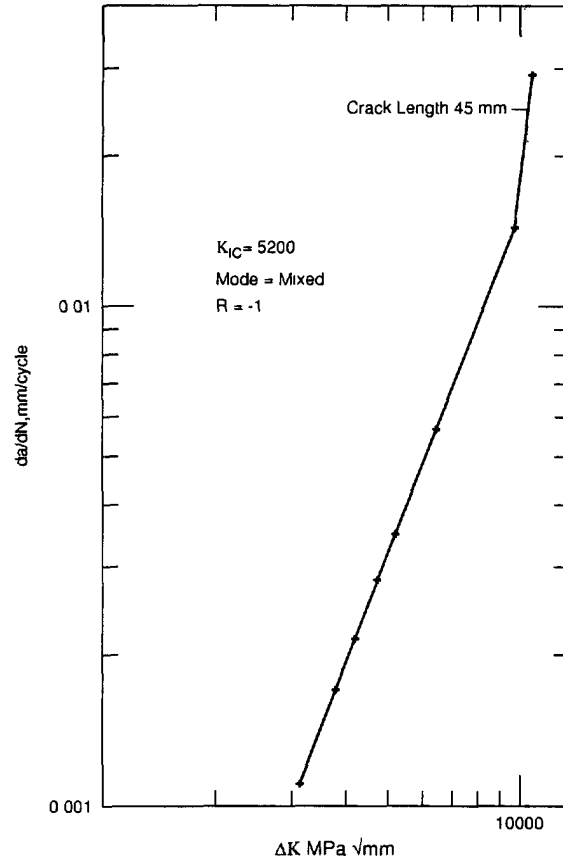
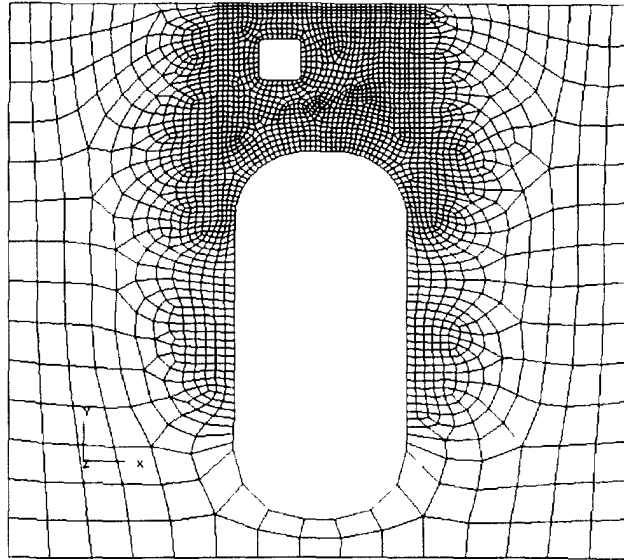


Figure 35: Crack Growth Rate to Failure for a Crack Originating at a Hole



*Figure 36: Finite Element Model of a Longitudinal Bulkhead Detail*

## 7 Crack Propagation and Turning in a Ship Structural Detail

---

A finite element model of a ship structural detail is shown in Figure 36. The model represents openings in a longitudinal bulkhead. The model has been simplified by eliminating the stiffeners and the reinforcing normally used around openings, as these components cannot be accounted for within current capability of the crack propagation analysis program. The stresses in the detail model were obtained from a MAESTRO global analysis of a finite element model of the ship (see Figure 37). It was subjected to a load consisting of applied bow and stern bending moments to cause sagging and hogging mode displacements. The detail was extracted from the MAESTRO finite element global model and the finite element mesh refined. The boundary conditions for the detail were extracted from the results of the MAESTRO analysis and were applied in the form of prescribed displacements. The stresses resulting from the applied boundary conditions were obtained by a finite element analysis using VAST and are shown in Figure 38.

The model of the detail was too large for efficient repetitive incremental modeling and analysis required for the crack growth propagation prediction. For this reason it was considered as the global model and an additional extraction was performed including mainly the region of high stress concentration. The local extracted portion is shown in Figure 39. The extracted local detail was remeshed, while maintain-

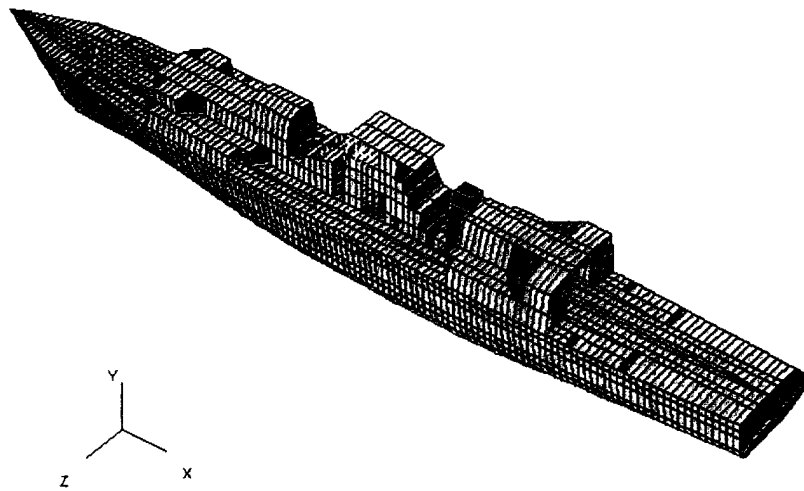


**Figure 37:** The MAESTRO Finite Element Model of a Ship from Which the Longitudinal Bulkhead Detail was Taken

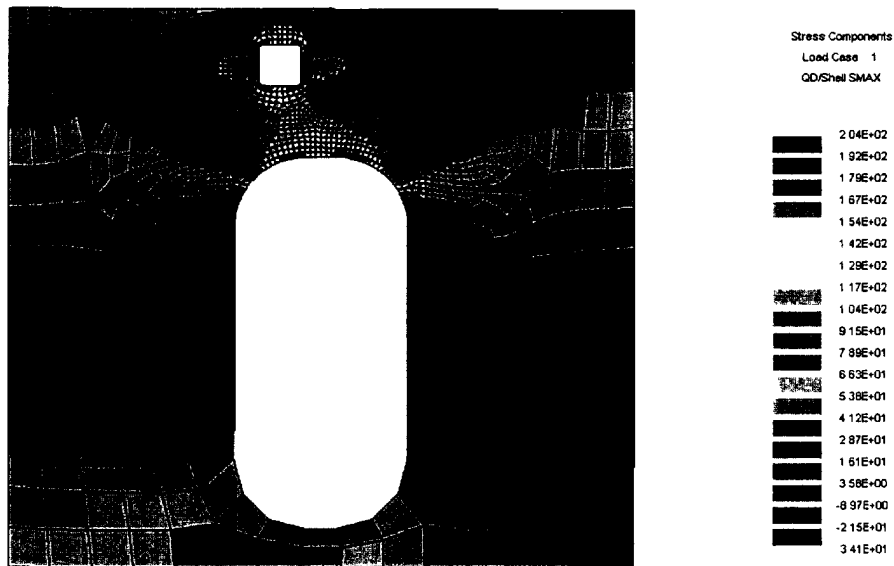


**Figure 38:** Maximum Constant Amplitude Stress Distribution in the Longitudinal Bulkhead Detail

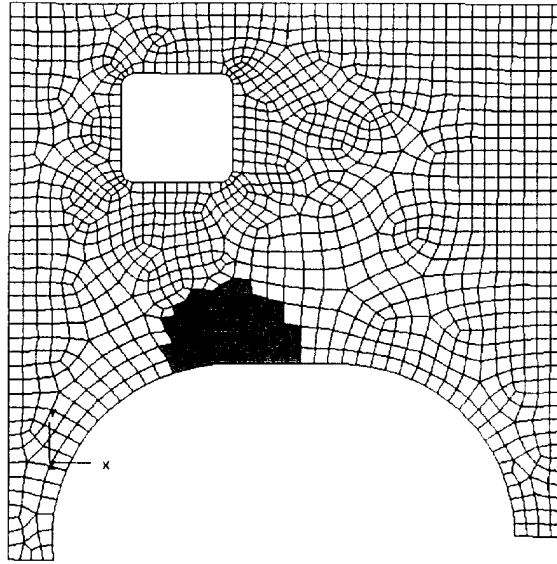


**Figure 39:** Local Portion with the Starting Crack Extracted from the Longitudinal Bulkhead Detail

ing the boundary node positions, to include the start of a crack. The remeshed model was reinserted into the global model and the boundary nodes at the interface between the global and local models were automatically identified and boundary conditions in the form of displacements were determined and automatically applied as shown in Figure 40. The VAST analysis was repeated at this stage as a top-down analysis to obtain the stresses and stress intensity factors in the local detail at the crack. The crack propagation was obtained by incrementally repeating this process at crack growth increments of 20 mm and remeshing the local detail to accommodate the change in crack length. The crack propagated without significant turning as shown in Figure 41. At this stage the stress intensity factor reached a maximum value of  $3155 \text{ MPa}\sqrt{\text{mm}}$ . This was well below the critical  $K_{Ic} = 5200 \text{ MPa}\sqrt{\text{mm}}$ . The crack growth versus the number of load cycles during propagation to a crack length of 320 mm is shown in Figure 42. The number of constant amplitude load cycles to produce the crack was estimated to be 25000. The analysis showed that the crack grew to meet the hole in the bulkhead. During its growth it did not reach the critical intensity factor at the crack tip thereby indicating there was no likelihood of a brittle fracture. The hole itself would help in arresting further crack growth.

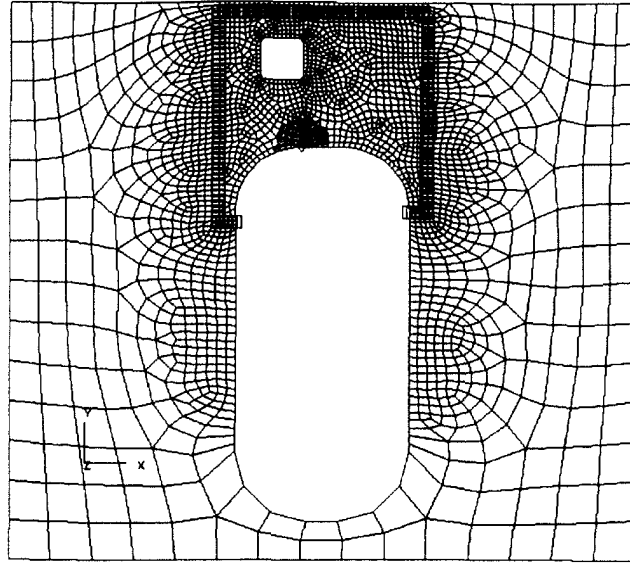
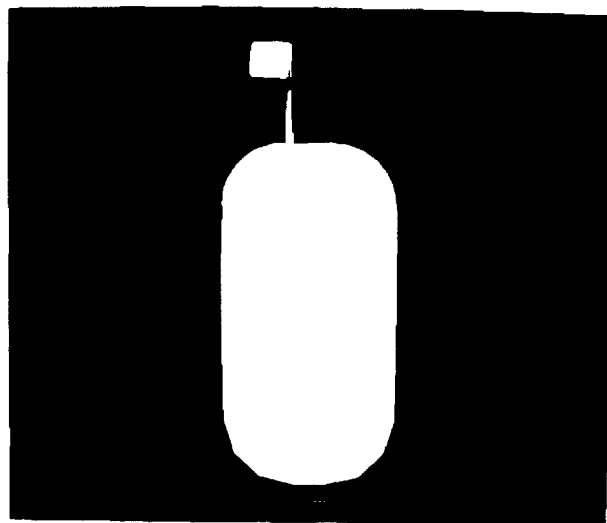


**Figure 40:** The Boundary Conditions Automatically Applied to the Boundaries Between the Local and Global Models



Stress Intensity Factors  
SIF1 3.155E+03  
SIF2 -7.814E+00

**Figure 41:** Propagation of the Crack in the Longitudinal Bulkhead

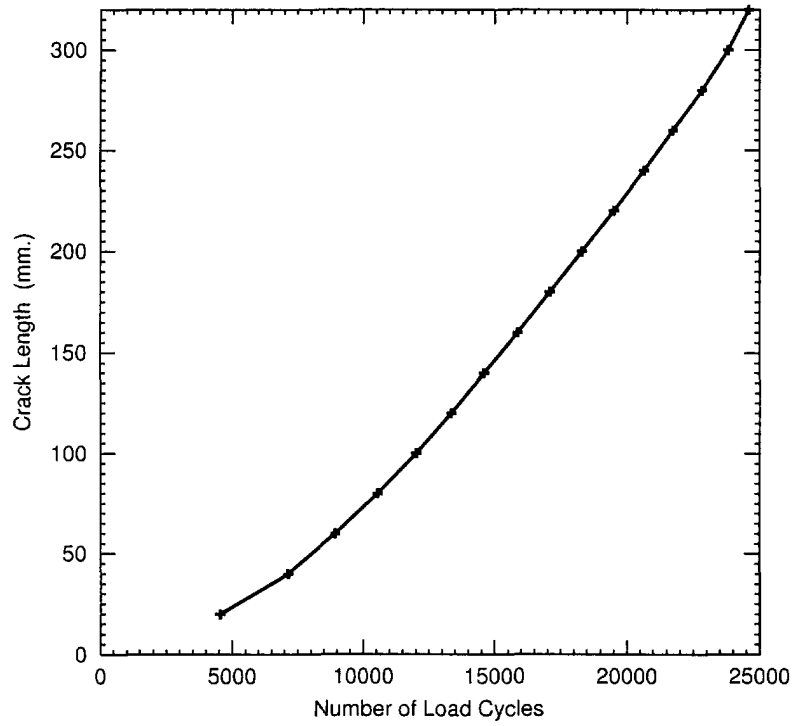


**Figure 42:** Growth of the Crack in the Longitudinal Bulkhead

## 8 Discussion

---

In preparation for the investigation of crack turning during propagation, the performances of VAST and its auxiliary programs LIFE3D and K1K2CRACK were assessed. The stress intensity factors produced by the crack tip element in VAST was shown to be in excellent agreement with values calculated using an equation reported to have an accuracy within 0.5 %. To obtain this agreement, at least 5 crack elements beyond the crack tip had to be used when modeling. It was also shown that there was good agreement with the calculated value, for crack length to failure under a constant amplitude load, with that obtained by incremental finite element analysis. The calculated value for the number of cycles to failure was shown to agree exactly with the value from finite element analysis using VAST and the program K1K2CRACK.

It is generally accepted that a crack will propagate mainly during the opening of the crack under a constant amplitude load and in a direction normal to the direction of principal stress. This was shown to be the case for an edged cracked plate under a tension load normal to the crack direction. The crack progressed straight across the plate without turning until just before fracture. It was shown, however, in the case of the pure shear loading of Mode II a horizontal centre crack will propagate by immediately turning  $81^\circ$  and will exhibit shear movement between the two surfaces.

Further investigation of crack turning showed there was no turning of a crack starting at the edge of a plate during its propagation under a constant amplitude Mode I load applied normal to the crack. When a crack, inclined at  $45^\circ$ , was situated at the center of the plate and subjected to a Mode I load, it propagated by initially turning through approximately  $45^\circ$  and then continued to propagate along a line normal to the tension load to the point of fracture. Crack turning did occur when an edge shear load was applied to the plate with an edge crack thus in effect creating a mixed mode situation. An edge cracked plate under tension, with a hole present, will propagate in a straight line unless the crack propagates very near the hole so that it will be affected by the stress concentrated at the hole. In which case the crack will turn towards the hole at the last stages of its growth.

The current crack analysis capabilities of the programs should be developed to include more complex geometries such as fillet welds and variable plate thickness. Variable amplitude loads should be accounted for. The ability to predict the growth of surface cracks through the plate thickness should also be included along with the ability to plot principal stress trajectories for better insight into crack growth direction.

## References

---

1. Paris P.C. and Erdogan F."A Critical Analysis of Crack Propagation Laws", Trans. ASME J. Basic Engng", 1963.
2. 'VIBRATION AND STRENGTH ANALYSIS PROGRAM(VAST):User's Manual', Martec Ltd., Halifax Nova Scotia, April 1997.
3. 'MG/DSA' Martec Ltd. Halifax Nova Scotia
4. 'LIFE3D' Martec Ltd. Halifax Nova Scotia
5. Peterson R.E.,'Stress Concentration Factors',John Wiley and Son, 1974.
6. Rolfe Stanley T., and Barsom John M.  
Fracture and Fatigue Control in Structures Prentice Hall Inc. New Jersey, 1977.
7. Meguid S.A., Engineering Fracture Mechanics, Elsevier Applied Science Publishers, London, 1989.
8. Dowling Norman E., Mechanical Behaviour of Materials Prentice Hall, New Jersey
9. Forman R.G., Kearney V.E., and Engle R.M., 'Numerical Analysis of Crack Propagation in Cyclic-loaded Structures' J. Basic Engng. Trans. ASME 89, pp.459-63,1967
10. K1K2CRACK, 'A Program for Estimating Crack Growth Direction', Martec Ltd., Halifax Nova Scotia
11. G.C.SIH, "Strain-energy-density Factor Applied to Mixed Mode Crack Problems" International Journal of Fracture, Vol 10, No. 3, Sept. 1974.

**UNCLASSIFIED**  
SECURITY CLASSIFICATION OF FORM  
(highest classification of Title, Abstract, Keywords)

<b>DOCUMENT CONTROL DATA</b>		
(Security classification of title, body of abstract and indexing annotation must be entered when the overall document is classified)		
<b>1 ORIGINATOR</b> (the name and address of the organization preparing the document. Organizations for whom the document was prepared, e.g. Establishment sponsoring a contractor's report, or tasking agency, are entered in section 8) <b>Defence Research Establishment Atlantic</b> <b>P.O. Box 1012</b> <b>Dartmouth, Nova Scotia, Canada B2Y 3Z7</b>	<b>2 SECURITY CLASSIFICATION</b> (overall security classification of the document including special warning terms if applicable)  <div style="text-align: center; font-size: large;"><b>Unclassified</b></div>	
<b>3 TITLE</b> (the complete document title as indicated on the title page. Its classification should be indicated by the appropriate abbreviation (S,C,R or U) in parentheses after the title) <b>A Procedure</b> <b>Investigation of Crack Turning in Fracture in Ship Structures</b>		
<b>4 AUTHORS</b> (Last name, first name, middle initial. If military, show rank, e.g. Doe, Maj John E.)  <b>Smith, Donald R.</b>		
<b>5 DATE OF PUBLICATION</b> (month and year of publication of document)  <b>July 2001</b>	<b>6a NO OF PAGES</b> (total containing information. Include Annexes, Appendices, etc.)  <div style="text-align: center; font-size: large;"><b>34</b></div>	<b>6b NO OF REFS</b> (total cited in document)  <div style="text-align: center; font-size: large;"><b>11</b></div>
<b>7 DESCRIPTIVE NOTES</b> (the category of the document, e.g. technical report, technical note or memorandum. If appropriate, enter the type of report, e.g. interim, progress, summary, annual or final. Give the inclusive dates when a specific reporting period is covered)  <b>DREA Contractor Report</b>		
<b>8 SPONSORING ACTIVITY</b> (the name of the department project office or laboratory sponsoring the research and development. Include address) <b>Defence Research Establishment Atlantic</b> <b>P.O. Box 1012</b> <b>Dartmouth, N.S. B2Y 3Z7</b>		
<b>9a PROJECT OR GRANT NO</b> (if appropriate, the applicable research and development project or grant number under which the document was written. Please specify whether project or grant)  <b>11gc-13</b>	<b>9b CONTRACT NO</b> (if appropriate, the applicable number under which the document was written)  <b>W7707-0-8234</b>	
<b>10a ORIGINATOR'S DOCUMENT NUMBER</b> (the official document number by which the document is identified by the originating activity. This number must be unique to this document)  <b>DREA CR 2001-067</b>	<b>10b OTHER DOCUMENT NOS</b> (Any other numbers which may be assigned this document either by the originator or by the sponsor)	
<b>11 DOCUMENT AVAILABILITY</b> (any limitations on further dissemination of the document, other than those imposed by security classification) <input checked="" type="checkbox"/> Unlimited distribution <input type="checkbox"/> Defence departments and defence contractors; further distribution only as approved <input type="checkbox"/> Defence departments and Canadian defence contractors; further distribution only as approved <input type="checkbox"/> Government departments and agencies; further distribution only as approved <input type="checkbox"/> Defence departments; further distribution only as approved <input type="checkbox"/> Other (please specify): Defence Departments of TTCP Countries		
<b>12 DOCUMENT ANNOUNCEMENT</b> (any limitation to the bibliographic announcement of this document. This will normally correspond to the Document Availability (11). However, where further distribution (beyond the audience specified in (11)) is possible, a wider announcement audience may be selected)  <b>Full, unlimited</b>		

**UNCLASSIFIED**  
SECURITY CLASSIFICATION OF FORM

**UNCLASSIFIED**SECURITY CLASSIFICATION OF FORM  
(highest classification of Title, Abstract, Keywords)

13. **ABSTRACT** (a brief and factual summary of the document. It may also appear elsewhere in the body of the document itself. It is highly desirable that the abstract of classified documents be unclassified. Each paragraph of the abstract shall begin with an indication of the security classification of the information in the paragraph (unless the document itself is unclassified) represented as (S), (C), (R), or (U). It is not necessary to include here abstracts in both official languages unless the text is bilingual)

AVAS

The ability to predict crack propagation in a ship structure by finite element analysis based on linear elastic fracture mechanics was investigated. The investigation showed that the stress intensity factor at the crack tip, the number of cycles of constant amplitude loading to reach the critical intensity factor, and the critical length of the crack could be accurately predicted. The investigation concentrated on the ability to predict crack turning during propagation. Cracks originating at a plate edge, at a hole, and in the centre of a plate were evaluated. The results showed that crack turning was most likely to occur under mixed mode loading combining shear and tension.

14. **KEYWORDS, DESCRIPTORS or IDENTIFIERS** (technically meaningful terms or short phrases that characterize a document and could be helpful in cataloguing the document. They should be selected so that no security classification is required. Identifiers, such as equipment model designation, trade name, military project code name, geographic location may also be included. If possible keywords should be selected from a published thesaurus, e.g. Thesaurus of Engineering and Scientific Terms (TEST) and that thesaurus-identified. If it not possible to select indexing terms which are Unclassified, the classification of each should be indicated as with the title)

crack propagation  
 ship structures  
 fatigue  
 fracture  
 crack tip  
 crack turning  
 stress intensity factor

**UNCLASSIFIED**

SECURITY CLASSIFICATION OF FORM

**Defence R&D Canada**

is the national authority for providing  
Science and Technology (S&T) leadership  
in the advancement and maintenance  
of Canada's defence capabilities.

**R et D pour la défense Canada**

est responsable, au niveau national, pour  
les sciences et la technologie (S et T)  
au service de l'avancement et du maintien des  
capacités de défense du Canada.

#516676

CA020011



[www.drdc-rddc.dnd.ca](http://www.drdc-rddc.dnd.ca)